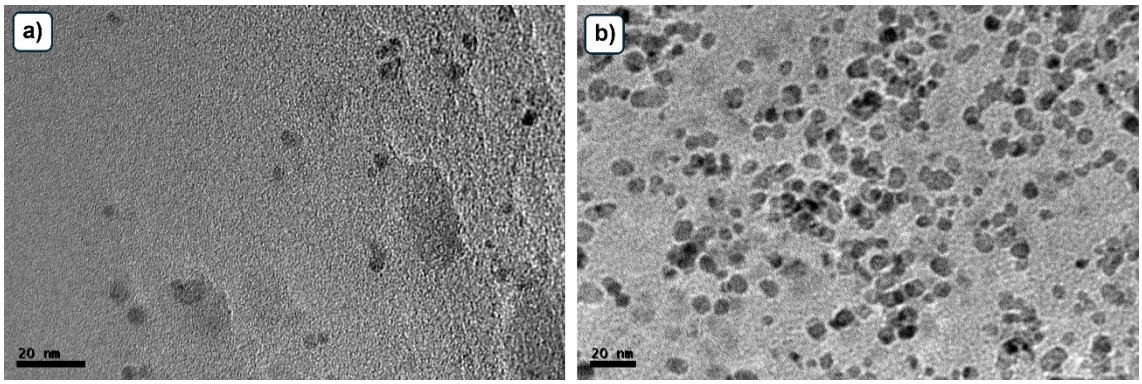

Figure S1: TEM images of the MRH hydrogels for concentrations of a) 0.0025 M and b) 0.1 M.

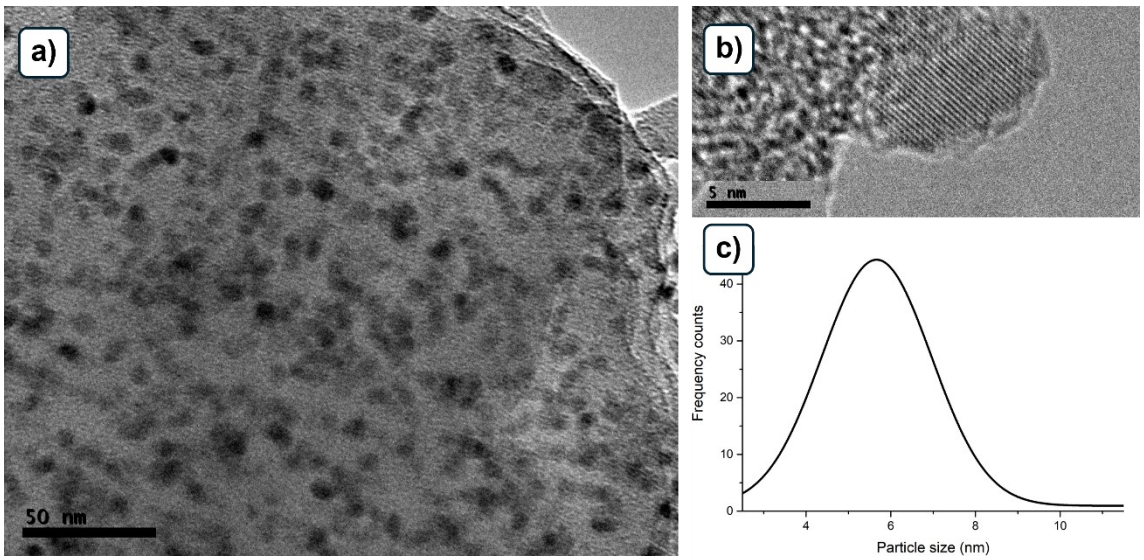

Figure S2: TEM image showing: a) TEM morphologies for the hydrogel MRH at 0.05M, b) image of the lattice patterns of the Fe_3O_4 crystal and c) the size distribution of NPs in that MRH hydrogel.

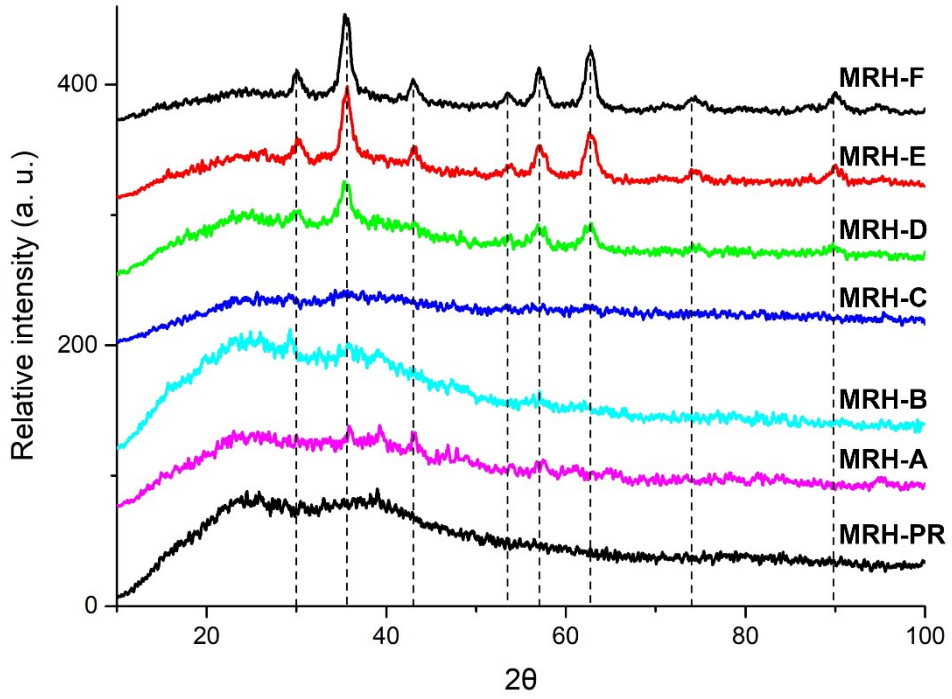

Figure S3a: PXRD patterns for MRH samples with various concentrations and pristine. Dashed lines corresponds to the indexed peaks for the Fe_3O_4 phase.

Position (2θ)	Height [cts]	FWHM Left (2θ)	d-spacing (Å)
29,98	16,79	0,79	2,98
35,59	53,12	0,94	2,52
43,01	14,24	0,79	2,10
53,49	8,25	0,94	1,71
57,03	27,32	0,47	1,62
62,75	37,71	0,71	1,48
74,20	4,97	0,09	1,28
89,87	9,85	0,09	1,09

Table S3b: Peak list of the MRH hydrogel with a concentration of 0.1M.

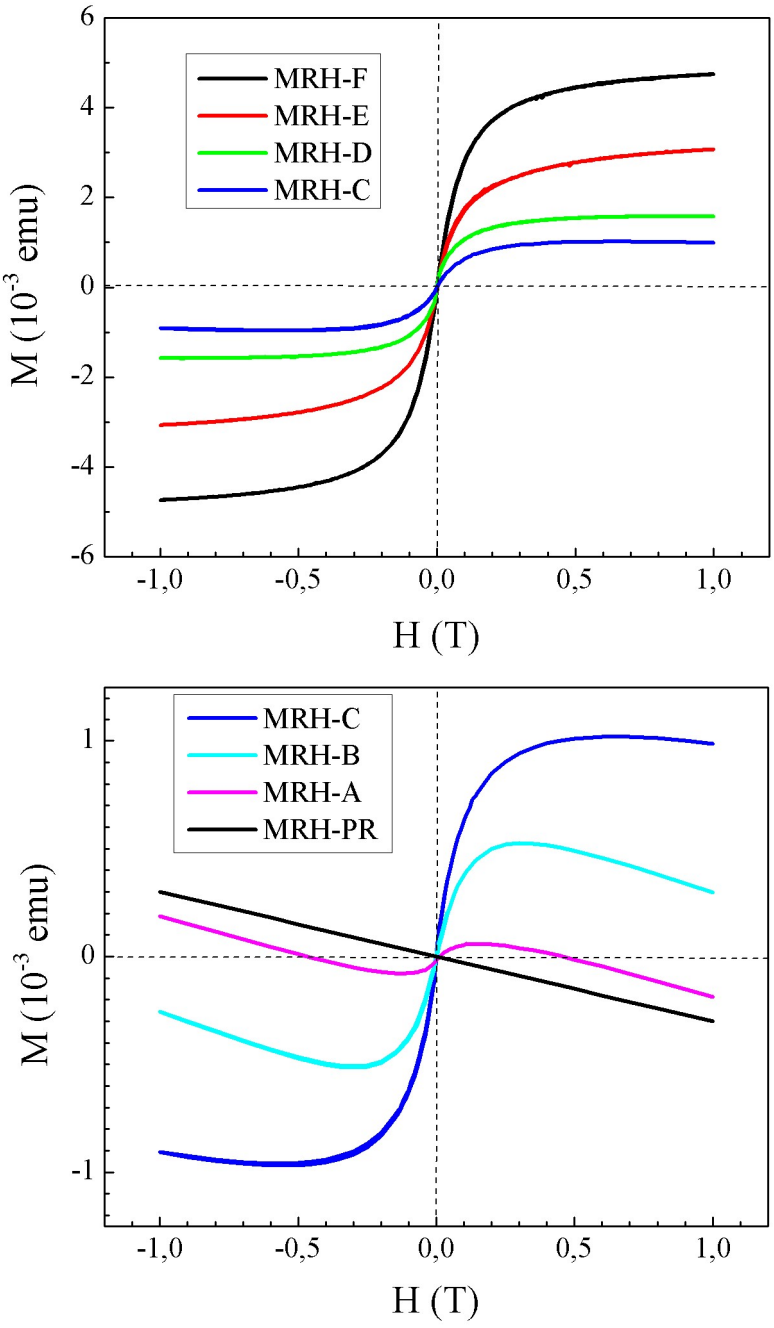

Figure S4: Magnetization raw data for MRH samples. Their corresponding NPs concentrations correlate with their names in both legends (see also the table in the manuscript). Those results have been split in two graphs to highlight the noticeable effect of the diamagnetic contribution to M in MRH samples with low NP concentrations (lower graph).

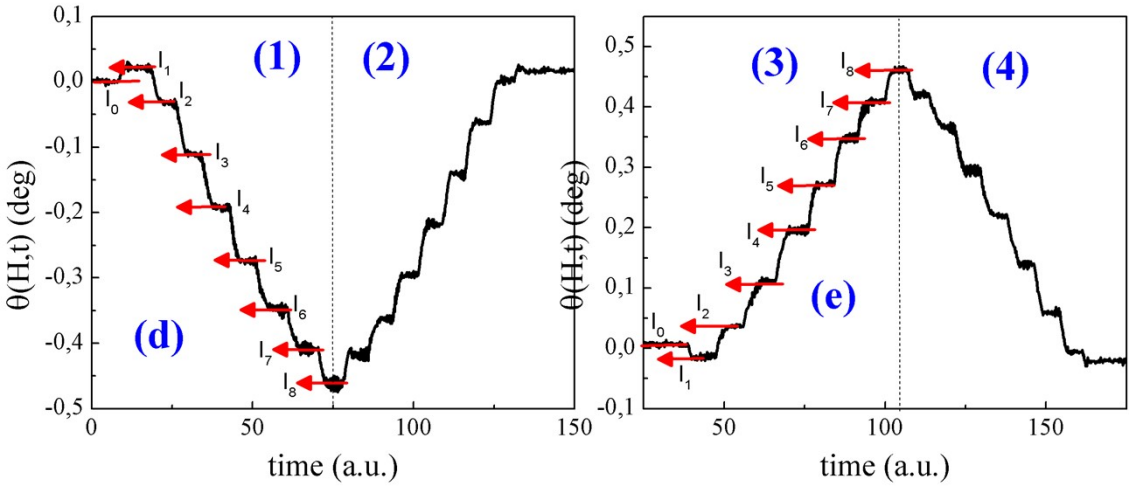

Figure S5.a: MOFE raw data for the MRH-F sample (plots (a) and (b) in the Fig. 2 of the resubmitted version)

1) The black line indicates the recorded azymuth of the transmitted light during the MOFE experiment.
2) I_0 to I_8 correspond to the values of the current source (I) circulating across the electromagnet. Each value can be converted to H units through the calibration curve of the electromagnet. These values are shown in the table below.
3) The H field was cycled between ± H_{max} at regular I steps. Its effect is seen in the corresponding steps of the azymuth of figure S4.
4) The whole MOFE experiment consisted in four regions as H ranged from: (1) zero to H_{max}, (2) H_{max} to zero, (3) zero to -H_{max} and (4) -H_{max} to zero.
5) The resulting set of (θ,H) data results in the (f) plot of the following figures panel. The same procedure is followed for all MRH samples, including the pristine MRH-PR sample, which its resulting graph Is the (c) plot in the following figure.

I (A)	H (mT)
0	0
0,5	88
1	178
1,5	266
2	352
2,5	427
3	488
3,5	539
4	577

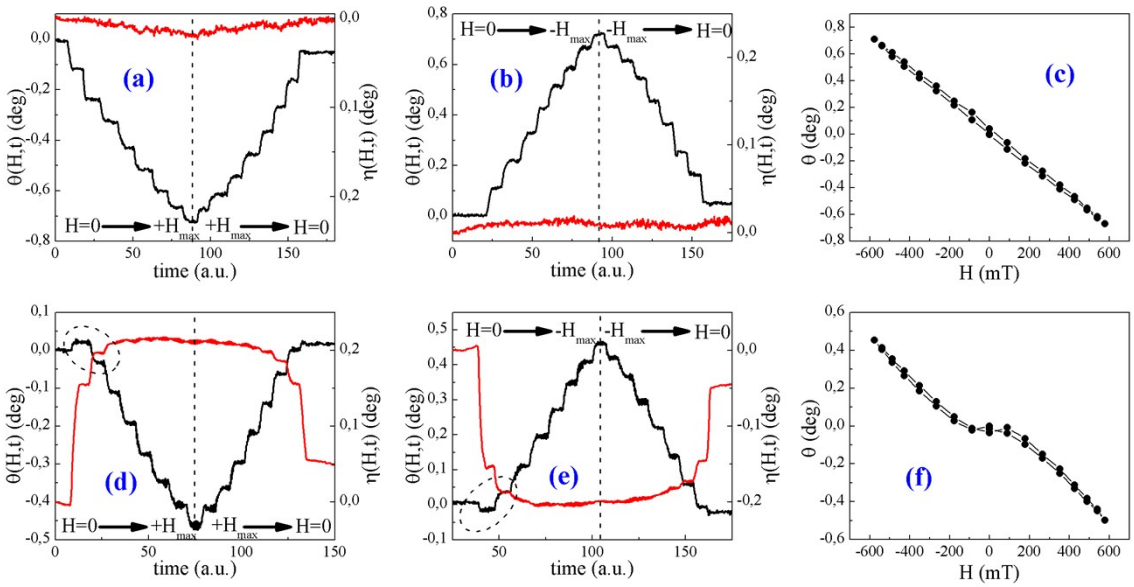

Figure S5.b: Upper row: (a) and (b) graphs show the time and field dependence of the azimuth (left, black line) and ellipticity (right, red line) of the SOP for the transmitted light through MRH-PR sample, and (c) graph corresponds to the field dependence of θ for the same sample. Lower row: (d-f) graphs show the same magnitudes for MRH-F sample. Circled data in graphs (d) and (e) are only intended to highlight the NPs response to increasing H in the low field range.

The data for the figure 3 in the manuscript, i.e. the MOFE, have calculated by subtracting the diamagnetic contribution (plot c in S5.b) to each magnetic MRH.

For instance, $\theta_{F,MRH\text{-}F} = \theta_{F,Plot(f)} - \theta_{F,Plot(c)}$

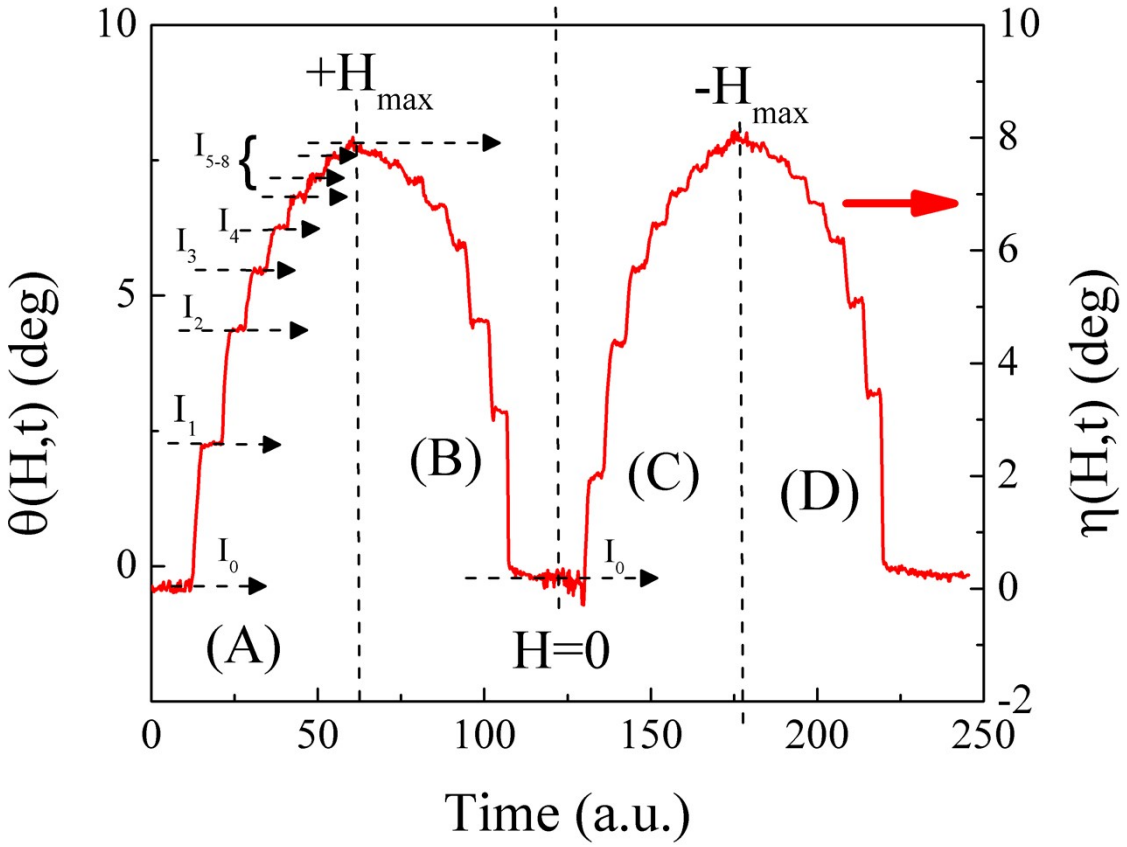

Figure S5.c: MOVE raw data for the MRH-F sample (from the figure 4 in the manuscript)

1) The red line indicates the recorded ellipticity of the transmitted light during the MOVE experiment.
2) I_0 to I_8 correspond to the values of the current source (I) circulating across the electromagnet. Each value can be converted to H units through the calibration curve of the electromagnet. These values are shown in the table below.
3) The H field was cycled between ± H_{max} at regular I steps. Its effect is seen in the corresponding steps of the ellipticity of figure S5.c.
4) The whole MOVE experiment consisted in four regions as H ranged from: (A) zero to H_{max}, (B) H_{max} to zero, (C) zero to $-H_{max}$ and (D) $-H_{max}$ to zero.
5) The resulting set of (η,H) data corresponds to the figure 5 in the manuscript. The same procedure is followed for all MRH samples.

I (A)	H (mT)
0	0
0,5	88
1	178
1,5	266
2	352
2,5	427
3	488
3,5	539
4	577